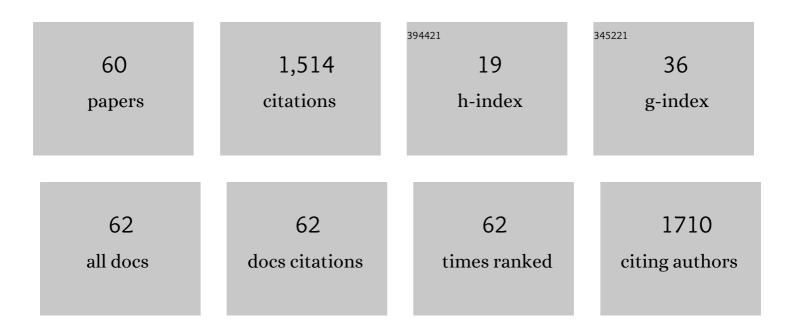


## List of Publications by Year in descending order

Source: https://exaly.com/author-pdf/5779706/publications.pdf Version: 2024-02-01



\A/FLLL

#	Article	IF	CITATIONS
1	Photothermal Diatomite/Carbon Nanotube Combined Aerogel for Highâ€Efficiency Solar Steam Generation and Wastewater Purification. Solar Rrl, 2022, 6, .	5.8	9
2	Accelerated Redox Conversion by CoMoS3/CoS Synergistic Interactions for High-Performance Lithium Sulfur Batteries. Journal of Electroanalytical Chemistry, 2022, , 116025.	3.8	5
3	Flexible and wearable strain sensors based on conductive hydrogels. Journal of Polymer Science, 2022, 60, 2663-2678.	3.8	45
4	Delayed autumnal leaf senescence following nutrient fertilization results in altered nitrogen resorption. Tree Physiology, 2022, 42, 1549-1559.	3.1	5
5	Enhanced performance of asymmetric supercapacitor based on NiZn-LDH@NiCoSe <sub>2</sub> electrode materials. Nanotechnology, 2022, 33, 295402.	2.6	16
6	The Effect of Elemental Doping on Nickel-Rich NCM Cathode Materials of Lithium Ion Batteries. Journal of Physical Chemistry C, 2022, 126, 151-159.	3.1	24
7	Compressible piezoresistive pressure sensor based on Ag nanowires wrapped conductive carbonized melamine foam. Applied Physics A: Materials Science and Processing, 2022, 128, 1.	2.3	14
8	Boosting Low-Temperature Resistance of Energy Storage Devices by Photothermal Conversion Effects. ACS Applied Materials & Interfaces, 2022, 14, 23400-23407.	8.0	6
9	Preparation and application of graphene-based wearable sensors. Nano Research, 2022, 15, 9850-9865.	10.4	20
10	Anti-inflammatory action of physalin A by blocking the activation of NF-κB signaling pathway. Journal of Ethnopharmacology, 2021, 267, 113490.	4.1	24
11	A wide temperature-tolerant hydrogel electrolyte mediated by phosphoric acid towards flexible supercapacitors. Chemical Engineering Journal, 2021, 413, 127446.	12.7	66
12	Biomimetic anti-freezing polymeric hydrogels: keeping soft-wet materials active in cold environments. Materials Horizons, 2021, 8, 351-369.	12.2	250
13	Reduced graphene oxide/g-C <sub>3</sub> N <sub>4</sub> modified carbon fibers for high performance fiber supercapacitors. New Journal of Chemistry, 2021, 45, 923-929.	2.8	16
14	Cascade Chan‣am Câ^'O Coupling/[3,3]â€Rearrangement of Arylhydroxylamines with Arylboronic Acids Toward NOBIN Analogues. Advanced Synthesis and Catalysis, 2021, 363, 1733-1738.	4.3	11
15	Low-Temperature-Resistant Flexible Solid Supercapacitors Based on Organohydrogel Electrolytes and Microvoid-Incorporated Reduced Graphene Oxide Electrodes. ACS Applied Materials & Interfaces, 2021, 13, 12432-12441.	8.0	44
16	Anti-inflammatory effects of three withanolides isolated from Physalis angulata L. in LPS-activated RAW 264.7 cells through blocking NF-κB signaling pathway. Journal of Ethnopharmacology, 2021, 276, 114186.	4.1	9
17	Significant efficiency enhancement of CdSe/CdS quantum-dot sensitized solar cells by black TiO2 engineered with ultrashort filamentating pulses. Applied Surface Science Advances, 2021, 6, 100142.	6.8	5
18	High coercivity Pr2Fe14B magnetic nanoparticles by a mechanochemical method. RSC Advances, 2021, 11, 12315-12320.	3.6	1

Wei Lu

#	Article	IF	CITATIONS
19	Reduced graphene oxide/polyaniline wrapped carbonized sponge with elasticity for energy storage and pressure sensing. New Journal of Chemistry, 2021, 45, 7860-7866.	2.8	11
20	In vitro anti-inflammatory activities of naucleoffieine H as a natural alkaloid from <i>Nauclea officinalis</i> Pierrc ex Pitard, through inhibition of the iNOS pathway in LPS-activated RAW 264.7 macrophages. Natural Product Research, 2020, 34, 2694-2697.	1.8	11
21	A photo-assisted rechargeable battery: synergy, compatibility, and stability of a TiO <sub>2</sub> /dye/Cu <sub>2</sub> S bifunctional composite electrode. Nanoscale, 2020, 12, 530-537.	5.6	35
22	Improved performance of quantum dot-sensitized solar cells by full-spectrum utilization. Superlattices and Microstructures, 2020, 148, 106730.	3.1	4
23	A facile synthetic strategy of free-standing holey graphene paper as sulfur host for high-performance flexible lithium sulfur batteries. Journal of Electroanalytical Chemistry, 2020, 876, 114728.	3.8	9
24	The g-C <sub>3</sub> N <sub>4</sub> Quantum Dot Decorated g-C <sub>3</sub> N <sub>4</sub> Sheet/Reduced Graphene Oxide Composite as Efficient Metal-Free Electrocatalyst for Oxygen Reduction Reaction. Journal of the Electrochemical Society, 2020, 167, 100534.	2.9	5
25	Boosting Power Conversion Efficiency of Quantum Dot-Sensitized Solar Cells by Integrating Concentrating Photovoltaic Concept with Double Photoanodes. Nanoscale Research Letters, 2020, 15, 188.	5.7	10
26	Fabrication and Electrochemical Performance of PVA/CNT/PANI Flexible Films as Electrodes for Supercapacitors. Nanoscale Research Letters, 2020, 15, 151.	5.7	56
27	Cobalt and nitrogen codoped carbon nanotubes derived from a graphitic C <sub>3</sub> N <sub>4</sub> template as an electrocatalyst for the oxygen reduction reaction. Nanoscale Advances, 2020, 2, 3963-3971.	4.6	6
28	Improved nucleation of AlN on <i>in situ</i> nitrogen doped graphene for GaN quasi-van der Waals epitaxy. Applied Physics Letters, 2020, 117, .	3.3	22
29	Neuron-like hierarchical manganese sulfide@Cu <sub>2</sub> S core/shell arrays on Ni foam as an advanced electrode for an asymmetric supercapacitor. CrystEngComm, 2020, 22, 6047-6056.	2.6	15
30	Synergistically Controlled Mechanism of Sodium Birnessite with a Larger Interlayer Distance for Fast Ion Intercalation toward Sodium-Ion Batteries. Journal of Physical Chemistry C, 2020, 124, 28431-28436.	3.1	11
31	<i>In situ</i> fabrication of Al surface plasmon nanoparticles by metal–organic chemical vapor deposition for enhanced performance of AlGaN deep ultraviolet detectors. Nanoscale Advances, 2020, 2, 1854-1858.	4.6	7
32	Transition-metal-free aerobic C–O bond formation via C–N bond cleavage. Organic Chemistry Frontiers, 2020, 7, 1077-1081.	4.5	22
33	Highly transparent and flexible graphitic C3N4 nanowire/PVA/PEDOT:PSS supercapacitors for transparent electronic devices. Functional Materials Letters, 2020, 13, 2051006.	1.2	0
34	The formation mechanism of voids in physical vapor deposited AlN epilayer during high temperature annealing. Applied Physics Letters, 2020, 116, .	3.3	28
35	Porous Carbon Networks Derived From Graphitic Carbon Nitride for Efficient Oxygen Reduction Reaction. Nanoscale Research Letters, 2019, 14, 249.	5.7	22
36	Synthesis of Three Dimensional Porous Carbon Materials Using g-C3N4 as Template for Supercapacitors. Journal of the Electrochemical Society, 2019, 166, A3564-A3569.	2.9	10

Wei Lu

#	Article	IF	CITATIONS
37	Three-Dimensional Carbon Nitride Nanowire Scaffold for Flexible Supercapacitors. Nanoscale Research Letters, 2019, 14, 98.	5.7	22
38	Plasma Treatment for Nitrogenâ€Doped 3D Graphene Framework by a Conductive Matrix with Sulfur for Highâ€Performance Li–S Batteries. Small, 2019, 15, e1804347.	10.0	97
39	Combined photoanodes of TiO <sub>2</sub> nanoparticles and {001}-faceted TiO <sub>2</sub> nanosheets for quantum dot-sensitized solar cells. New Journal of Chemistry, 2019, 43, 8551-8556.	2.8	5
40	(3R, 7R)-7-Acetoxyl-9-Oxo-de-O-Methyllasiodiplodin, a Secondary Metabolite of Penicillium Sp., Inhibits LPS-Mediated Inflammation in RAW 264.7 Macrophages through Blocking ERK/MAPKs and NF-κB Signaling Pathways. Inflammation, 2019, 42, 1463-1473.	3.8	6
41	Carbon nanoparticle template assisted formation of mesoporous TiO2 photoanodes for quantum dot-sensitized solar cells. New Journal of Chemistry, 2019, 43, 5374-5381.	2.8	6
42	Cascade Approach to Highly Functionalized Biaryls by a Nucleophilic Aromatic Substitution with Arylhydroxylamines. Organic Letters, 2019, 21, 2894-2898.	4.6	38
43	Flexible and Stretchable Energy Storage Device Based on Ni(HCO <sub>3</sub> ) <sub>2</sub> ÂNanosheet Decorated Carbon Nanotube Electrodes for Capacitive Sensor. Journal of the Electrochemical Society, 2019, 166, A4014-A4019.	2.9	5
44	Enhanced performance of flexible ultraviolet photodetectors based on carbon nitride quantum dot/ZnO nanowire nanocomposites. Materials Research Express, 2019, 6, 045002.	1.6	11
45	Identification of β-carboline and canthinone alkaloids as anti-inflammatory agents but with different inhibitory profile on the expression of iNOS and COX-2 in lipopolysaccharide-activated RAW 264.7 macrophages. Journal of Natural Medicines, 2019, 73, 124-130.	2.3	20
46	Highly Dispersed Surfactant-Free Amorphous NiCoB Nanoparticles and Their Remarkable Catalytic Activity for Hydrogen Generation from Ammonia Borane Dehydrogenation. Catalysis Letters, 2018, 148, 1739-1749.	2.6	9
47	A sea cucumber-like BiOBr nanosheet/Zn <sub>2</sub> GeO <sub>4</sub> nanorod heterostructure for enhanced visible light driven photocatalytic activity. Materials Research Express, 2018, 5, 015009.	1.6	4
48	Reduced graphene oxide (RGO)/Cu2S composite as catalytic counter electrode for quantum dot-sensitized solar cells. Electrochimica Acta, 2018, 277, 50-58.	5.2	61
49	Three-dimensional reduced-graphene/MnO <sub>2</sub> prepared by plasma treatment as high-performance supercapacitor electrodes. Materials Research Express, 2018, 5, 065504.	1.6	8
50	Antiâ€ʻinflammatory action of ambuic acid, a natural product isolated from the solid culture of Pestalotiopsis�neglecta, through blocking ERK/JNK mitogenâ€ʻactivated protein kinase signaling pathway. Experimental and Therapeutic Medicine, 2018, 16, 1538-1546.	1.8	10
51	Improved performance of quantum dot-sensitized solar cells based on TiO2 nanoparticle/nanorod photoanodes. Journal of Alloys and Compounds, 2017, 715, 337-343.	5.5	5
52	Graphitic carbon nitride modified {001}-faceted TiO2 nanosheet photoanodes for efficient quantum dot sensitized solar cells. Superlattices and Microstructures, 2017, 109, 860-868.	3.1	16
53	β1,6 GlcNAc branches-modified protein tyrosine phosphatase alpha enhances its stability and promotes focal adhesion formation in MCF-7Âcells. Biochemical and Biophysical Research Communications, 2017, 482, 1455-1461.	2.1	5
54	Ionic liquid polymer functionalized carbon nanotubes-doped poly(3,4-ethylenedioxythiophene) for highly-efficient solid-phase microextraction of carbamate pesticides. Journal of Chromatography A, 2016, 1444, 42-49.	3.7	61

Wei Lu

#	Article	IF	CITATIONS
55	Plasma-induced, nitrogen-doped graphene-based aerogels for high-performance supercapacitors. Light: Science and Applications, 2016, 5, e16130-e16130.	16.6	152
56	Morphological control of RGO/CdS hydrogels for energy storage. CrystEngComm, 2016, 18, 1090-1095.	2.6	36
57	Wnt/β-catenin signaling induces the transcription of cystathionine-γ-lyase, a stimulator of tumor in colon cancer. Cellular Signalling, 2014, 26, 2801-2808.	3.6	62
58	β1,6 GlcNAc Branches-Modified PTPRT Attenuates Its Activity and Promotes Cell Migration by STAT3 Pathway. PLoS ONE, 2014, 9, e98052.	2.5	9
59	The van der Waals Epitaxy of Highâ€Quality Nâ€Polar Gallium Nitride for Highâ€Response Ultraviolet Photodetectors with Polarization Electric Field Modulation. Advanced Electronic Materials, 0, , 2100759.	5.1	5
60	A 3D honeycomb graphene structure for wearable piezoresistive pressure sensor with high sensitivity. Journal of Materials Science: Materials in Electronics, 0, , 1.	2.2	2